JOURNAL OF Materials CHEMISTRY

High-temperature synthesis, crystal structure, optical properties, and magnetism of the carbidonitridosilicates $Ho_2[Si_4N_6C]$ and $Tb_2[Si_4N_6C]$

Henning A. Höppe, Gunter Kotzyba, Rainer Pöttgen and Wolfgang Schnick*

Department of Chemistry, University of Munich (LMU), Butenandtstr. 5–13 (block D) D-81377 Munich, Germany. E-mail: wsc@cup.uni-muenchen.de

Received 20th July 2001, Accepted 4th October 2001
First published as an Advance Article on the web 1st November 2001

The novel carbidonitridosilicates $Ho_2[Si_4N_6C]$ and $Tb_2[Si_4N_6C]$ were obtained by the reaction of the respective lanthanoid metal with carbon and $Si(NH)_2$ in a radiofrequency furnace at the temperature of 1700 °C. According to the single-crystal structure analysis of $Ho_2[Si_4N_6C]$ ($P2_1/c$, $Z=4$, $a=593.14(1)$, $b=989.74(1)$, $c=1188.59(2)$ pm, $\beta=119.58(4)°$, $R1=0.0355$, $wR2=0.0879$, 2187 F^2 values, 119 parameters) the compound contains a condensed network of corner-sharing star like $[C(SiN_3)_4]$ units. The holmium ions are situated in channels along [100]. The UV–VIS absorption spectrum of $Ho_2[Si_4N_6C]$ shows the typical Ho^{3+} absorption bands. The spectroscopic results show that the 4f states remain almost unaffected by the coordination sphere and thus it is impossible to distinguish between the two crystallographic sites of Ho^{3+} in the UV–VIS spectrum. Magnetic susceptibility measurements of $Tb_2[Si_4N_6C]$ and $Ho_2[Si_4N_6C]$ show Curie–Weiss behaviour above 150 K with experimental magnetic moments of 9.57(6) μ_B/Tb and 10.27(4) μ_B/Ho. The Weiss constants are −15(1) K and −11(1) K for the terbium and holmium compounds, respectively. Down to 2 K no magnetic ordering could be detected. The magnetization curves at 2 K show an increase of the magnetization with increasing flux density, indicating partial parallel spin alignments. At 5 T the magnetizations reach values of 4.15(5) μ_B/Tb and 4.75(5) μ_B/Ho, respectively.

Introduction

Recently, quaternary nitrogen atoms ($N^{[4]}$) have been identified in the nitridosilicate series $MYb[Si_4N_7]$ (M = Ba, Sr, Eu)[1–3] and in $Er_6Si_{11}N_{20}O$ type oxonitridosilicates[4,5] which connect four neighbouring tetrahedral Si centres. All previously investigated nitridosilicate network structures are built up from alternating Si and N, with the nitrogen atoms being negatively polarized. In contrast the unprecedented structural motif NSi_4 exhibits an ammonium character and thus the $N^{[4]}$ atoms carry a formally positive charge. It seems promising to replace the fourfold coordinated nitrogen by carbon in order to introduce carbon bridges into nitridosilicate network structures. This replacement may lead to better mechanical properties because of the higher covalency of the Si–C bond compared with Si–N. So far no crystalline Si–(C/N) network structures with anionic carbon are known, however recently the silicon carbodiimides SiC_2N_4 and Si_2CN_4 have been found. These compounds are structurally related to SiO_2 and Si_2N_2O, respectively, with a substitution of O by NCN groups.[6,7] In this context the new super-hard cubic compound BC_2N has to be mentioned as well.[8]

The novel compound $Ho_2[Si_4N_6C]$ by serendipity was obtained in very low yield as a byproduct of $Ho_6[Si_{11}N_{20}O]$ when the synthesis was carried out in graphite crucibles. After stoichiometric addition of graphite to the reaction mixture $Ho_2[Si_4N_6C]$ was obtained as a single-phase product.

We chose the term "carbidonitridosilicate" to emphasise the character of the $Si^{4+}(N^{3-},C^{4-})$ network, *i.e.* a substitution of N^{3-} by C^{4-} in nitridosilicates. The prefix carbo would suggest a positively charged carbon atom as found in carbodiimides and would mean that carbon substitutes Si^{4+} and acts thus as a C^{4+} like in the intensively discussed silicon carbonitrides.

Experimental procedure

Synthesis of silicon diimide "$Si(NH)_2$"

Using "$Si(NH)_2$" instead of the relatively inert Si_3N_4 as starting material proved to be advantageous for the synthesis of nitridosilicates and this also holds for sions and sialons.[9–11] "$Si(NH)_2$" was obtained by ammonolysis of $SiCl_4$ in NH_3 (−78 °C) followed by a thermal treatment at 600 °C under an atmosphere of NH_3 (see eqn. (1)).

$$SiCl_4 + 6NH_3 \xrightarrow[NH_3\ \text{atmosphere}]{-78\,^\circ C} Si(NH)_2 + 4NH_4Cl \xrightarrow[NH_3\ \text{atmosphere}]{600\,^\circ C,\ -NH_4Cl} Si(NH)_2 \quad (1)$$

A detailed description of the synthesis of "$Si(NH)_2$" is given in ref. 11. "$Si(NH)_2$" was obtained as an X-ray amorphous and relatively undefined but reactive product which is converted to amorphous Si_3N_4 at temperatures above 900 °C. It is an important precursor for the technical production of Si_3N_4 ceramics.[12]

Synthesis of $Ho_2[Si_4N_6C]$ and $Tb_2[Si_4N_6C]$

In an argon filled glove box 44.8 mg (0.272 mmol) holmium metal (Chempur, 99.9%), 50.0 mg silicon diimide and 1.2 mg (0.10 mmol) graphite (Merck, purest) were thoroughly mixed and transferred into a graphite crucible (Conradty Mechanical & Electrical GmbH, spec. B 497 XN). The synthesis of $Ho_2[Si_4N_6C]$ (see eqn. (2)) was performed in a previously described radiofrequency furnace under a purified nitrogen atmosphere. The mixture was heated to 900 °C within 5 min

 DOI: 10.1039/b106533p

and maintained at this temperature for 25 min before further heating to 1600 °C within 12 h. Then the temperature was raised to 1700 °C in 30 h and cooled down to room temperature within 30 min. More details about the experimental setup are given in ref. 11 and 13. $Ho_2[Si_4N_6C]$ was obtained as coarsely crystalline yellowish or pink powder (see optical properties).

$$2Ho + 4Si(NH)_2 + C \xrightarrow[N_2,\ r.f.\ furnace]{1700\,^{\circ}C} Ho_2[Si_4N_6C] + N_2 + 4H_2 \quad (2)$$

By an analogous synthesis with 39.5 mg (0.249 mmol) terbium metal (Chempur, 99.9%), 58.6 mg silicon diimide and 19.5 mg (1.63 mmol) graphite (Merck, purest) in a tungsten crucible the terbium compound $Tb_2[Si_4N_6C]$ was obtained.

The quantitative elemental analysis (Pascher, Remagen) was found to fit well to the theoretical values (in parentheses): Ho 61.6 weight% (61.4%), Si 20.0% (20.8%), N 15.5% (15.6%), C 2.0% (2.2%).

UV–VIS measurements

For the measurements of UV–VIS absorption spectra in reflection geometry a Hitachi U-3501 spectrophotometer was used. The spectra were recorded at room temperature between 300 nm and 700 nm. Below 300 nm the background absorption of the object slide on which the samples were fixed grew rapidly.

Magnetic measurements

Magnetic susceptibility measurements were performed on polycrystalline and single-phase samples (6.288 mg $Tb_2[Si_4N_6C]$ and 12.22 mg $Ho_2[Si_4N_6C]$, respectively) by use of a MPMS *XL* SQUID magnetometer (Quantum Design, Inc.) at temperatures between 2 and 300 K and with magnetic flux densities up to 5 T. The measurements were carried out in thin-walled silica tubes.

Crystal structure analysis and lattice energy calculations

X-Ray diffraction data of the title compound $Ho_2[Si_4N_6C]$ were collected on a Kappa CCD area detector diffractometer (Nonius) equipped with a rotating anode. According to the observed extinction conditions of the monoclinic lattice (all reflections $h0l$ with $l=2n$, $0k0$ with $k=2n$ and $00l$ with $l=2n$) the space group $P2_1/c$ (no. 14) was chosen; because of the apparent similarity of the powder diffraction patterns of $Ho_2[Si_4N_6C]$ and $BaYb[Si_4N_7]$ (space group $P6_3mc$, no. 186) a symmetry reduction was taken into account and therefore the space group $P2_1$ (no. 4) was also considered.

The structure solution and refinement was only possible choosing space group $P2_1/c$. The crystal structure of $Ho_2[Si_4N_6C]$ was solved by direct methods using SHELXTL[14] and refined with anisotropic displacement parameters for all atoms. The relevant crystallographic data and further details of the X-ray data collection are summarised in Table 1. Table 2 shows the positional and displacement parameters for all atoms. In Table 3 selected interatomic distances and angles are listed. Furthermore all reflections detected by X-ray powder diffraction (Stoe Stadi P) of single-phase $Ho_2[Si_4N_6C]$ were indexed and their observed intensities are in good agreement with the calculated diffraction patterns based on the single-crystal data. The Rietveld refinement of the lattice parameters was performed with the program GSAS.[15] The powder diffraction pattern of $Ho_2[Si_4N_6C]$ is shown in Fig. 1.

Table 1 Crystallographic data of $Ho_2[Si_4N_6C]$ and $Tb_2[Si_4N_6C]$ (e.s.d.s in parentheses)

Crystal Data	
$Ho_2[Si_4N_6C]$	
$M=2153.16$ g mol^{-1}	$F(000)=952$
Monoclinic	$\rho=5.892$ g cm^{-3}
space group $P2_1/c$ (No. 14)	Mo-K_α radiation
$a=593.14(1)$ pm	$\lambda=71.073$ pm
$b=989.74(1)$ pm	$\mu=26.61$ mm^{-1}
$c=1188.59(2)$ pm	$T=293(2)$ K
$\beta=119.58(4)^\circ$	Needle
$V=606.82(2)\times10^6$ pm^3	$0.150\times0.050\times0.040$ mm^3
$Z=4$	Yellow/pink (depending on light)
Data Collection	
Nonius KappaCCD area detector	Measured octants: all
Absorption correction: numerical (ψ-scans)	$h=-8\rightarrow8$
$T_{min}=0.0282$; $T_{max}=0.1377$	$k=-14\rightarrow14$
$R_{int}=0.0905$	$l=-17\rightarrow15$
$2\theta_{max}=64.9^\circ$	2187 independent reflections
	2131 observed reflections ($F_o^2\geqslant2\sigma(F_o^2)$)
Refinement	
Refinement on F^2	Program used to refine structure: SHELXL-97
$R1=0.0355$ (all data)	$w^{-1}=\sigma^2F_o^2+(xP)^2+yP$; $P=(F_o^2+2F_c^2)/3$
$wR2=0.0879$ (all data)	Weighting scheme (x/y) 0.0316/7.0620
GooF = 1.276	Extinction coefficient: 0.0031(2)
31309 measured reflections	Min. residual electron density: -4.715 e Å^{-3}
119 parameters	Max. residual electron density: 2.205 e Å^{-3}
Powder Diffraction (Rietveld Refinement of the lattice parameters)	
$Ho_2[Si_4N_6C]$	$Tb_2[Si_4N_6C]$
$a=592.57(2)$ pm	$a=594.47(5)$ pm
$b=989.41(3)$ pm	$b=993.19(3)$ pm
$c=1187.16(4)$ pm	$c=1193.48(4)$ pm
$\beta=119.691(2)^\circ$	$\beta=120.066(9)^\circ$
$V=604.65(4)\times10^6$ pm^3	$V=609.84(8)\times10^6$ pm^3
$wR_P=0.056$	$wR_P=0.060$
$R_P=0.044$	$R_P=0.048$
$R_F^2=0.041$	$R_F^2=0.059$
$R_F=0.031$	$R_F=0.037$
$\chi^2=5.87$	$\chi^2=1.48$
845 reflections ($2\theta_{max}=50.0^\circ$)	1794 reflections ($2\theta_{max}=60.0^\circ$)

Table 2 Atomic coordinates and anisotropic displacement parameters for $Ho_2[Si_4N_6C]$ (e.s.d.s in parentheses). All atoms occupy the 4e site of space group $P2_1/c$

atom	x	y	z	U_{11}	U_{22}	U_{33}	U_{23}	U_{13}	U_{12}	U_{eq}
Ho(1)	0.33162(5)	0.56439(3)	0.09506(3)	99(2)	132(2)	99(2)	−22(1)	59(2)	−32(1)	106(1)
Ho(2)	0.66039(5)	0.41486(3)	0.41946(3)	95(2)	90(2)	88(2)	9(1)	57(2)	20(1)	86(1)
Si(1)	0.0051(4)	0.4804(2)	0.2492(2)	86(7)	69(7)	91(7)	7(6)	55(6)	−5(6)	77(3)
Si(2)	0.1654(4)	0.2137(2)	0.4207(2)	74(8)	89(8)	76(7)	−8(6)	45(6)	0(6)	76(3)
Si(3)	0.2018(4)	0.2059(2)	0.1763(2)	89(7)	86(8)	83(7)	−3(6)	55(6)	−4(6)	80(3)
Si(4)	0.6767(4)	0.2281(2)	0.1590(2)	80(8)	86(7)	86(8)	−3(6)	50(7)	2(6)	80(3)
N(1)	0.043(2)	0.2110(8)	0.0089(6)	136(26)	256(30)	73(21)	−11(21)	76(20)	−85(23)	145(11)
N(2)	0.059(2)	0.0456(6)	0.3995(6)	83(21)	87(22)	117(22)	23(18)	56(18)	4(18)	93(9)
N(3)	0.241(2)	0.0356(6)	0.2234(6)	112(22)	70(21)	128(22)	1(18)	69(19)	8(18)	99(9)
N(4)	0.507(2)	0.2910(7)	0.0016(6)	70(21)	153(24)	110(22)	33(19)	34(18)	−11(19)	115(9)
N(5)	0.517(2)	0.2646(6)	0.2452(6)	83(23)	124(25)	143(24)	−18(18)	71(20)	−28(18)	111(10)
N(6)	0.699(1)	0.0532(6)	0.1373(6)	60(20)	93(23)	109(22)	14(17)	26(18)	4(17)	95(9)
C(1)	0.022(2)	0.2916(7)	0.2519(6)	68(23)	40(21)	121(24)	2(19)	48(20)	1(18)	76(9)

The anisotropic temperature factor is given as $\exp[-2\pi^2(U_{11}h2a^*2+\ldots+2U_{13}hla^*c^*)]$. U_{eq} is defined as one third of the trace of the orthogonalized U_{ij} tensor.

Table 3 Selected interatomic distances/pm and angles/° for $Ho_2[Si_4N_6C]$ (e.s.d.s in parentheses)

Ho(1)	–N(4)$^{[2]}$	231.9(6)
	–N(2)$^{[2]}$	234.3(5)
	–N(2)$^{[2]}$	235.8(5)
	–N(3)$^{[2]}$	240.2(5)
	–N(5)$^{[2]}$	257.9(6)
	–Ho(1)	366.48(6)
	–Ho(2)	366.57(4)
	–Ho(1)	389.57(6)
Ho(2)	–N(1)$^{[2]}$	233.3(6)
	–N(6)$^{[2]}$	233.9(5)
	–N(5)$^{[2]}$	234.2(6)
	–N(3)$^{[2]}$	237.5(5)
	–N(6)$^{[2]}$	250.2(5)
	–N(4)$^{[2]}$	261.0(6)
	–Ho(1)	347.45(4)
	–Ho(1)	366.57(4)
	–Ho(2)	370.44(6)
	–Ho(2)	388.86(6)
Si(1)	–N(3)$^{[2]}$	173.1(6)
	–N(2)$^{[2]}$	173.8(6)
	–N(6)$^{[2]}$	175.2(6)
	–C(1)$^{[4]}$	187.1(6)
Si(2)	–N(1)$^{[2]}$	171.5(6)
	–N(2)$^{[2]}$	175.3(6)
	–N(4)$^{[2]}$	176.2(6)
	–C(1)$^{[4]}$	191.3(6)
Si(3)	–N(5)$^{[2]}$	173.1(6)
	–N(1)$^{[2]}$	173.1(6)
	–N(3)$^{[2]}$	175.5(6)
	–C(1)$^{[4]}$	189.8(6)
Si(4)	–N(5)$^{[2]}$	174.1(6)
	–N(4)$^{[2]}$	174.4(6)
	–N(6)$^{[2]}$	176.6(6)
	–C(1)$^{[4]}$	189.3(6)
C(1)	–Si(1)$^{[4]}$	187.1(6)
	–Si(4)$^{[4]}$	189.3(6)
	–Si(3)$^{[4]}$	189.8(6)
	–Si(2)$^{[4]}$	191.3(6)
Si–C$^{[4]}$–Si		104.7(3)–118.5(3)
Si–N$^{[2]}$–Si		111.9(3)–124.1(3)
N$^{[2]}$–Si–N$^{[2]}$		103.3(3)–113.5(3)
C$^{[4]}$–Si–N$^{[2]}$		105.7(3)–113.2(3)

CCDC reference number 412000. See http://www.rsc.org/suppdata/jm/b1/b106533p/ for crystallographic files in CIF or other electronic format.

The lattice parameters of isotypic $Tb_2[Si_4N_6C]$ were also obtained from a Rietveld refinement.[15] As expected the larger

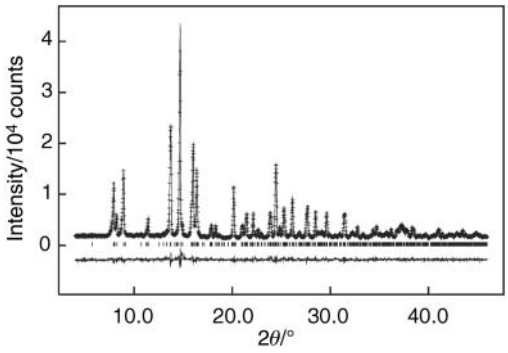

Fig. 1 Powder diffraction pattern of $Ho_2[Si_4N_6C]$, Mo-$K_{\alpha 1}$ radiation.

Tb^{3+} ions (as compared to Ho^{3+}) lead to a three-dimensional expansion of approximately 3–5% per axis of the unit cell.

$RE_2[Si_4N_6C]$ (RE = Tb, Ho) crystallise in a new structure type which can be derived from the $BaYb[Si_4N_7]$ structure by chemical twinning (see under crystallographic classification). Recently, Thompson *et al.*[16] postulated $La_2[Si_4N_6C]$ with the orthorhombic lattice parameters $a = 10.1276(10)$, $b = 10.5667(16)$ and $c = 6.0321(6)$ pm, directly deriving from the structure of $BaYb[Si_4N_7]$. $Ho_2[Si_4N_6C]$ and $Tb_2[Si_4N_6C]$ crystallise unequivocally in a monoclinic cell and exhibit a significantly different structure.

Due to their identical electronic configurations and their very similar atomic form factors the unequivocal differentiation of N^{3-}/C^{4-} by X-ray diffraction is not reliable. Therefore the assignment of the Ho, Si, N and C atoms to their crystallographic positions in $Ho_2[Si_4N_6C]$ was checked by lattice energy calculations using the MAPLE concept (MAPLE = Madelung Part of Lattice Energy).[17–19] The results of these calculations are summarised in Table 4. They are in very good agreement with the expected data.

Further details of the crystal structure investigations reported in this paper may be obtained from the Fachinformationszentrum Karlsruhe, D-76344 Eggenstein-Leopoldshafen, Germany, by quoting the depository number CSD – 412000.

Results and discussion of the structure refinement

$Ho_2[Si_4N_6C]$ consists of a three-dimensional network of condensed SiN_3C tetrahedra. The carbon atom connects four Si tetrahedral centres to form a star like unit $[C(SiN_3^{[2]})_4]$ (Figs. 2 and 3). These units are connected sharing their N$^{[2]}$ atoms (which link two tetrahedral Si centres) to form two types of layers perpendicular to [001] with diametrical orientation of the SiN_3C tetrahedra (Fig. 4). Along [001] these two types of layers

Table 4 Results of the MAPLE calculations for $Ho_2[Si_4N_6C]$ and increment calculations in kJ mol^{-1}; Δ = difference

Ho(1)	Ho(2)	Si(1)	Si(2)	Si(3)	Si(4)	N(1)	N(2)	N(3)	N(4)	N(5)	N(6)	C(1)
4347	4547	9932	9785	9772	9764	5445	5502	5480	5429	5433	5475	9429

MAPLE(2 HoN + Si_3N_4 + $SiC_{wurtzite}$)/kJ mol^{-1}	MAPLE($Ho_2Si_4N_6C$)/kJ mol^{-1}
90497	90383, Δ = 0.1%

Typical partial MAPLE values (in kJ mol^{-1}): Ho^{3+}: 3900–4550; Si^{4+}: 9000–10200; N^{3-}: 5000–6000; C^{4-}: 8700–9700

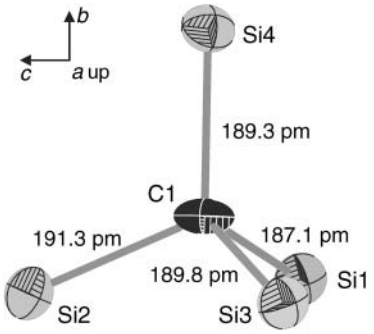

Fig. 2 CSi_4 tetrahedron, view along [100], the displacement ellipsoids represent 95% probability.

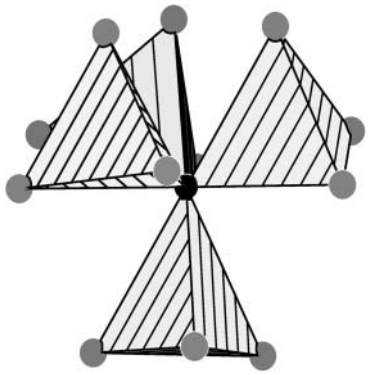

Fig. 3 Star like unit $[C(SiN_3)_4]$. The SiN_3C tetrahedra are shown as closed polyhedra. Carbon and nitrogen are shown as solid black and grey circles, respectively.

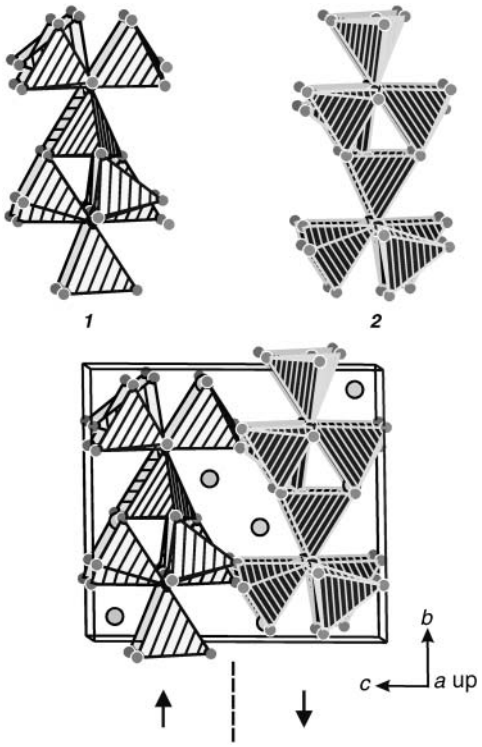

Fig. 4 View of the $Ho_2[Si_4N_6C]$ structure along [100]; layers ***1*** and ***2*** perpendicular to [001] formed by $C(SiN_3)_4$ units show "chemical twinning" by inversion at the centre of the unit cell; the SiN_3C tetrahedra are shown as closed polyhedra. Carbon and nitrogen are shown as solid black and grey circles, respectively. The metal atoms are shown as grey circles with black rings; the arrows indicate the diametrical orientation of both layers.

are alternately connected by further $N^{[2]}$ atoms like chemical twins (Fig. 4) to build the three-dimensional condensed network $^3_\infty[Si_4^{[4]}N_6^{[2]}C_1^{[4]6-}]$. By this chemical twinning the polar character of the $^3_\infty[Si_4^{[4]}N_6^{[2]}N_1^{[4]5-}]$ network in $MYb[Si_4N_7]$ with M = Sr, Ba, Eu is lost. Therefore, $Ho_2[Si_4N_6C]$ exhibits no SHG (second harmonic generation) activity in contrast to $MYb[Si_4N_7]$.[20]

The Si–N bond lengths (171.5(6) pm–176.6(6) pm) are in the typical range for nitridosilicates and the Si–C distances (187.1(6) pm–191.3(6) pm) agree well with those in wurtzite type silicon carbide (188 pm–190 pm)[21] and in $U_3Si_2C_2$ which contains a Si–C dumbbell (193(2) pm).[22] The carbon atom is tetrahedrally coordinated by four silicon atoms (Fig. 2). The Si–C–Si angles vary between 104.7(3)° and 118.5(3)°, the Si–$N^{[2]}$–Si angles range between 111.9(3)° and 124.0(3)° and the $N^{[2]}$–Si–$N^{[2]}$ angles between 103.3(3)°–113.5(3)°.

The Ho^{3+} ions are situated in channels formed by 6-rings along [100] as shown in Fig. 4. The Ho–N coordination distances vary in the range 231.9(6)–257.9(6) pm for Ho1 and 233.3(6)–261.0(6) pm for Ho2. Ho1 is coordinated by five nitrogen atoms and Ho2 by six (distorted octahedron), respectively (Fig. 5). The observed distances are in fair agreement with the coordination situation found in holmium nitrides (228–254 pm).[23]

Crystallographic classification

The network of $BaYb[Si_4N_7]$ was characterised as a stacking variant of wurtzite type AlN.[1,2] By systematic elimination of Si 6-ring channels along [100] are formed. The metal atoms are situated in these channels. The close structural relationship between $BaYb[Si_4N_7]$ and $Ho_2[Si_4N_6C]$ is emphasised by comparing the frequency distribution (*i.e.* the cycle-class sequence[24] for $n = 1, 2, 3...$) of Si_nX_n ring sizes (X = N, C) of

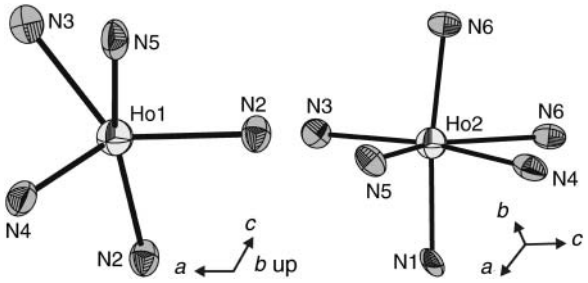

Fig. 5 Coordination of the holmium atoms in $Ho_2[Si_4N_6C]$, the displacement ellipsoids represent 95% probability.

Table 5 Comparison of the frequency distribution (*i.e.* the cycle-class sequence[24] for $n=1, 2, 3...$) of Si_nX_n ring sizes (X = N, C) in $Ho_2[Si_4N_6C]$ and $BaYb[Si_4N_7]$, respectively

Si_nX_n rings; $n=$	1	2	3	4	5	6	7	8	9	10
$Ho_2[Si_4N_6C]$	—	0	16	0	0	16	96	312	824	2076
$BaYb[Si_4N_7]$	—	0	8	0	0	8	48	156	412	1038

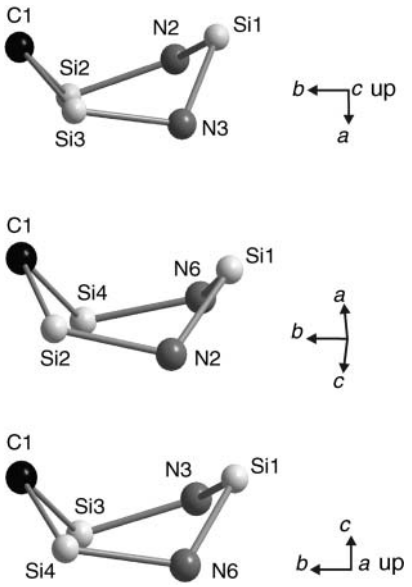

Fig. 6 Si_3N_2C rings in $Ho_2[Si_4N_6C]$.

both networks (Table 5). According to the differing unit cell contents ($Z=2$ for $MYb[Si_4N_7]$ and $Z=4$ for $Ho_2[Si_4N_6C]$) the cycle-class sequences of both structure types are related by a factor of two.

The network structure of $[Si_4N_6C]^{6-}$ can be derived from this arrangement by substitution of all $N^{[4]}$ by $C^{[4]}$ and by chemical twinning[25] perpendicular to [001] performing a symmetry operation on an inversion centre. In the resulting structure layers of $[C(SiN_3)_4]$ units with diametrical orientation alternate along [001] (Fig. 4). In $BaYb[Si_4N_7]$, analogously to the wurtzite structure type, the Si_3N_3 rings are found to be in a chair conformation perpendicular to the *c* axis and in a boat conformation along the *c* axis. Due to the twinning all Si_3N_2C rings in $RE_2[Si_4N_6C]$ exhibit a slightly distorted boat or half boat conformation, respectively (Fig. 6). Since the boat conformation is more appropriate for ionic networks, it is thus favourable for the herein described $[Si_4N_6C]^{6-}$ network, as the higher charges (C^{4-} compared with N^{3-}) are better compensated.

Optical properties

Nitridosilicates have proven to be suitable host lattices for high temperature stable phosphors such as $Ba_2Si_5N_8:Eu$ or $LaSi_3N_5:Eu$.[26,27] Ho^{3+} is an interesting rare earth ion for laser emission in the infrared range of 2 and 2.9 μm,[28] and recently the optical transitions of Ho^{3+} in YAG were investi- gated.[29]

The $^5I_8$ ground state of Ho^{3+} has the electronic configuration [Xe] $4f^{10}$. The UV–VIS absorption spectrum of $Ho_2[Si_4N_6C]$ (Fig. 7) shows characteristic groups of absorptions in the visible range corresponding to $4f^{10}\rightarrow4f^{10}$ transitions of the trivalent holmium ions. Table 6 shows the strongest observed transitions. The assignment was made according to the well known energy level scheme of free Ho^{3+} ions.[30] These transitions occur at the typical values and indicate that the

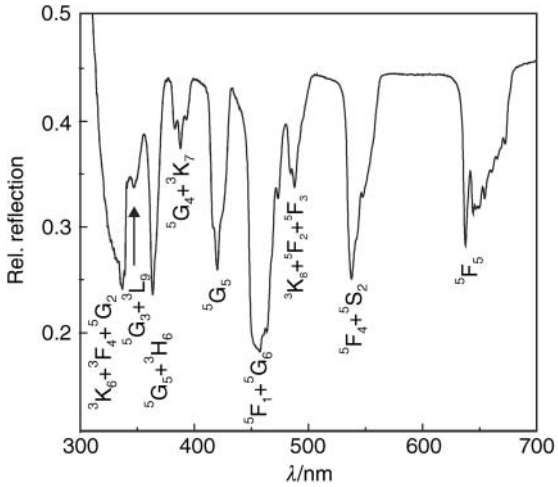

Fig. 7 UV–VIS absorption spectrum of $Ho_2[Si_4N_6C]$; the assigned transitions are marked.

Table 6 The absorption band energies for the strongest assigned transitions in $Ho_2[Si_4N_6C]$ and in free Ho^{3+} ions between 300 nm and 700 nm

Absorption	λ/nm	$Ho_2[Si_4N_6C]$ Energy/ 10^3 cm^{-1}	Free Ho^{3+} (ref. 30) Energy/ 10^3 cm^{-1}
$^5I_8\rightarrow{}^3K_6+{}^3F_4+{}^5G_2$	336	29.8	30.0–30.8
$^5I_8\rightarrow{}^5G_3+{}^3L_9$	347	28.8	28.8–29.0
$^5I_8\rightarrow{}^5G_5+{}^3H_6$	363	27.5	27.6–27.7
$^5I_8\rightarrow{}^5G_4+{}^3K_7$	388	25.8	25.8–26.1
$^5I_8\rightarrow{}^5G_5$	420	23.8	23.9
$^5I_8\rightarrow{}^5F_1+{}^5G_6$	457	21.9	22.1–22.4
$^5I_8\rightarrow{}^3K_8+{}^5F_2+{}^5F_3$	488	20.5	20.6–21.3
$^5I_8\rightarrow{}^5F_4+{}^5S_2$	542	18.5	18.4–18.6
$^5I_8\rightarrow{}^5F_5$	647	15.5	15.5

4f states remain almost unaffected by the two quite different coordination spheres of Ho^{3+} in $Ho_2[Si_4N_6C]$ (Fig. 5).

As observed under UV light $Ho_2[Si_4N_6C]$ exhibits a yellowish colour while under light of longer wavelength it looks pink. This fact can be easily explained by the UV–VIS absorption spectrum where two strong absorption bands at 450–470 nm and 535–550 nm, respectively, are observed. Above 700 nm up to 1100 nm no absorption bands could be detected.

Magnetic measurements

Recently we started a systematic investigation of the magnetic properties of rare earth containing nitridosilicates and oxonitridoaluminosilicates (sialons). An interesting example is the 13 K ferromagnet $Eu_2Si_5N_8$.[31]

The temperature dependence of the inverse magnetic susceptibilities of $Tb_2[Si_4N_6C]$ and $Ho_2[Si_4N_6C]$ is presented in the upper plots of Figs. 8 and 9. Above 150 K $Tb_2[Si_4N_6C]$ and $Ho_2[Si_4N_6C]$ show Curie–Weiss behaviour with experimental magnetic moments of 9.57(6) μ_B/Tb and 10.27(4) μ_B/Ho. These experimentally determined values are close to the values of 9.72 μ_B and 10.61 μ_B for the free Tb^{3+} and Ho^{3+} ions.[32] The paramagnetic Curie temperatures (Weiss constants) of −15(1) K and −11(1) K were determined by linear extrapolation of the high-temperature parts of the $1/\chi$ *vs.* *T* plots to $1/\chi=0$. The negative values are indicative of predominant antiferromagnetic interactions, however, the low-field and low-temperature measurements (middle of Fig. 8 and inset of Fig. 9) gave no indication of magnetic ordering down to 2 K.

The magnetization curve for $Tb_2[Si_4N_6C]$ at 2 K (Fig. 8)

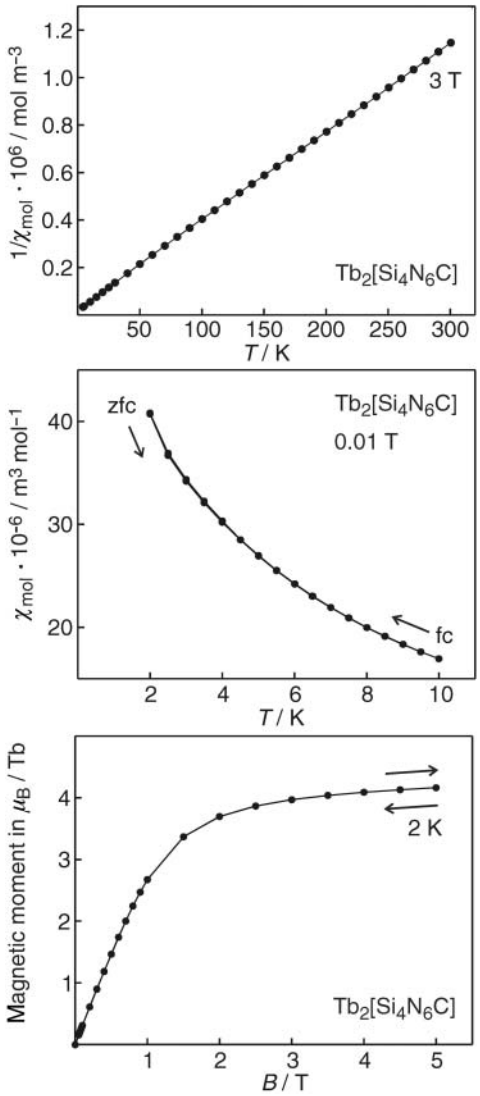

Fig. 8 Magnetic properties of $Tb_2[Si_4N_6C]$. The upper plot shows the temperature dependence of the inverse magnetic susceptibility at 3 T. In the middle the low-temperature susceptibility at 0.01 T measured in zero-field-cooling (zfc) and field-cooling (fc) modes is presented. The magnetization *vs.* external field dependence at 2 K is shown at the bottom.

shows an increase of the magnetization with increasing flux density, indicating partial reorientation of the magnetic moments towards parallel spin alignments. The magnetization at the highest obtainable field of 5 T is 4.15(5) μ_B/Tb which is significantly smaller than the saturation magnetization of 9 μ_B/Tb according to $\mu_{sm(calc)} = g \cdot J\ \mu_B$.[32] Similar magnetization behaviour is observed for $Ho_2[Si_4N_6C]$ (Fig. 9). With decreasing temperature (from 15 to 2 K), the magnetization isotherms become steeper. At 2 K the magnetization is 4.75(5) μ_B/Ho at 5 T, also smaller than $\mu_{sm(calc)} = 10\ \mu_B$/Ho.

Outlook

The formal substitution of fourfold coordinated nitrogen by carbon leads to the novel phases $Ho_2[Si_4N_6C]$ and $Tb_2[Si_4N_6C]$. Recently, we obtained further isotypic phases with RE = Gd, Dy, Er and Tm which will be reported elsewhere. Apparently the range of composition of nitridosilicates can be extended by the substitution of N by C leading to carbidonitridosilicates. In the quasi-ternary system metal nitride–Si_3N_4–SiC several further crystalline compounds should occur which may exhibit interesting materials properties.

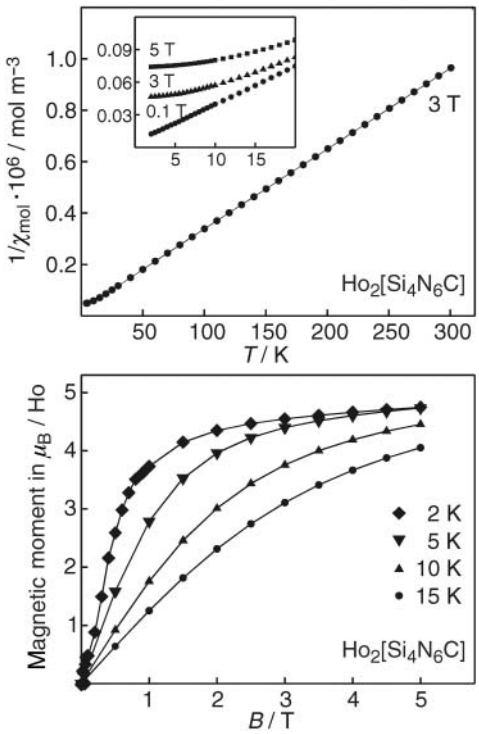

Fig. 9 Magnetic properties of $Ho_2[Si_4N_6C]$. The temperature dependence of the inverse magnetic susceptibility at 3 T is presented in the upper plot. The low temperature behaviour at different magnetic fields is shown in the inset. The magnetization *vs.* external field dependence at various temperatures is plotted below.

Acknowledgements

The authors thank Dr. Holger Piotrowski for the data collection on the Kappa CCD area detector system. This work was supported by the Fonds der Chemischen Industrie and especially by the Deutsche Forschungsgemeinschaft (Schwerpunktprogramm "Nitridobrücken" and Gottfried-Wilhelm-Leibniz-Programm).

References

1 H. Huppertz and W. Schnick, *Angew. Chem., Int. Ed. Engl.*, 1996, **35**, 1983.
2 H. Huppertz and W. Schnick, *Z. Anorg. Allg. Chem.*, 1997, **623**, 212.
3 H. Huppertz and W. Schnick, *Acta Crystallogr., Sect. C*, 1997, **53**, 1751.
4 M. Woike and W. Jeitschko, *J. Solid State Chem.*, 1997, **129**, 312.
5 K. Köllisch, H. A. Höppe, H. Huppertz, M. Orth and W. Schnick, *Z. Anorg. Allg. Chem.*, 2001, **627**, 1371.
6 R. Riedel, A. Greiner, G. Miehe, W. Dressler, H. Fuess, J. Bill and F. Aldinger, *Angew. Chem., Int. Ed. Engl.*, 1997, **36**, 603.
7 R. Riedel, E. Kroke, A. Greiner, A. O. Gabriel, L. Ruwisch, J. Nicolich and P. Kroll, *Chem. Mater.*, 1998, **10**, 2964.
8 V. Solozhenko, D. Andrault, G. Fiquet, M. Mezouar and D. R. Rubie, *Appl. Phys. Lett.*, 2001, **78**, 1385.
9 W. Schnick, T. Schlieper, H. Huppertz, K. Köllisch, M. Orth, R. Bettenhausen, B. Schwarze and R. Lauterbach, *Phosphorus Sulfur Relat. Elem.*, 1997, **124/125**, 163.
10 W. Schnick and H. Huppertz, *Chem. Eur. J.*, 1997, **3**, 679.
11 W. Schnick, H. Huppertz and R. Lauterbach, *J. Mater. Chem.*, 1999, **9**, 289.
12 H. Lange, G. Wötting and G. Winter, *Angew. Chem., Int. Ed. Engl.*, 1991, **30**, 1579.
13 T. Schlieper, W. Milius and W. Schnick, *Z. Anorg. Allg. Chem.*, 1995, **621**, 1380.
14 G. M. Sheldrick, SHELXTL, V 5.10 Crystallographic System, Bruker AXS Analytical X–ray Instruments Inc., Madison, WI, 1997.
15 R. B. von Dreele and A. C. Larson, General Structure Analysis System, Los Alamos National Laboratory Report LAUR 86-748, 1990.

16 K. Liddell and D. P. Thompson, *J. Mater. Chem.*, 2001, **11**, 507.
17 R. Hoppe, *Angew. Chem., Int. Ed. Engl.*, 1966, **5**, 95.
18 R. Hoppe, *Angew. Chem., Int. Ed. Engl.*, 1970, **9**, 25.
19 R. Hübenthal, MAPLE, Program for the Calculation of the Madelung Part of Lattice Energy, University of Gießen, Germany, 1993
20 H. Huppertz, PhD Thesis, University of Bayreuth, 1997.
21 R. F. Adamsky and K. M. Merz, *Z. Kristallogr.*, 1959, **111**, 350.
22 R. Pöttgen, D. Kaczorowski and W. Jeitschko, *J. Mater. Chem.*, 1993, **3**, 253.
23 N. E. Brese and M. O'Keeffe, *Struct. Bonding*, 1992, **79**, 307.
24 W. E. Klee, *Z. Kristallogr.*, 1987, **179**, 67.
25 S. Andersson, *Angew. Chem., Int. Ed. Engl.*, 1983, **22**, 69.
26 H. A. Höppe, H. Lutz, P. Morys, W. Schnick and A. Seilmeier, *J. Phys. Chem. Solids*, 2000, **61**, 2001.
27 K. Uheda, H. Takizawa, T. Endo, H. Yamane, M. Shimeda, C.-M. Wang and M. Mitomo, *J. Lumin.*, 2000, **87–89**, 967.
28 D. W. Hart, M. Jani and N. P. Barnes, *Opt. Lett.*, 1996, **21**, 728.
29 M. Malinowski, Z. Frukacz, M. Szuflinska, A. Wnuk and M. Kaczkan, *J. Alloys Compd.*, 2000, **300–301**, 389.
30 W. T. Carnall, P. R. Fields and K. Rajnak, *J. Chem. Phys.*, 1968, **49**, 4424.
31 H. A. Höppe, H. Trill, B. D. Mosel, H. Eckert, G. Kotzyba, R. Pöttgen and W. Schnick, *J. Phys. Chem. Solids*, 2001, **62**, in press.
32 A. Szytuła and J. Leciejewicz, *Handbook of Crystal Structures and Magnetic Properties of Rare Earth Intermetallics*, CRC Press, Boca Raton, FL, 1994.